environmental microbiology

Environmental Microbiology (2012) **14**(11), 2998–3012 doi:10.1111/j.1462-2920.2012.02876.x

Microbial cell budgets of an Arctic glacier surface quantified using flow cytometry

T. D. L. Irvine-Fynn,[1]* A. Edwards,[2] S. Newton,[3] H. Langford,[4,5] S. M. Rassner,[1] J. Telling,[6] A. M. Anesio[6] and A. J. Hodson[4,7]

[1]*Institute of Geography and Earth Science (IGES), Aberystwyth University, Aberystwyth, SY23 3DB, UK.*

[2]*Institute of Biological, Environmental and Rural Sciences (IBERS), Aberystwyth University, Aberystwyth, SY23 3DA, UK.*

[3]*Research Core Facility, The Medical School, University of Sheffield, Sheffield, S10 2RX, UK.*

[4]*Department of Geography, University of Sheffield, Sheffield, S10 2TN, UK.*

[5]*Kroto Research Institute, Department Civil and Structural Engineering, University of Sheffield, Sheffield, S3 7HQ, UK.*

[6]*School of Geographical Sciences, University of Bristol, Bristol, BS8 1SS, UK.*

[7]*Arctic Geology, University Centre on Svalbard (UNIS), PO Box 156, 9171 Longyearbyen, Norway.*

Summary

Uncertainty surrounds estimates of microbial cell and organic detritus fluxes from glacier surfaces. Here, we present the first enumeration of biological particles draining from a supraglacial catchment, on Midtre Lovénbreen (Svalbard) over 36 days. A stream cell flux of 1.08×10^7 cells m^{-2} h^{-1} was found, with strong inverse, non-linear associations between water discharge and biological particle concentrations. Over the study period, a significant decrease in cell-like particles exhibiting 530 nm autofluorescence was noted. The observed total fluvial export of ~ 7.5×10^{14} cells equates to 15.1–72.7 g C, and a large proportion of these cells were small (< 0.5 μm in diameter). Differences between the observed fluvial export and inputs from ice-melt and aeolian deposition were marked: results indicate an apparent storage rate of 8.83×10^7 cells m^{-2} h^{-1}. Analysis of surface ice cores revealed cell concentrations comparable to previous studies (6×10^4 cells ml^{-1}) but, critically, showed no variation with depth in the uppermost 1 m. The physical retention and growth of particulates at glacier surfaces has two implications: to contribute to ice mass thinning through feedbacks altering surface albedo, and to potentially seed recently deglaciated terrain with cells, genes and labile organic matter. This highlights the merit of further study into glacier surface hydraulics and biological processes.

Received 27 June, 2012; revised 16 August, 2012; accepted 17 August, 2012. *For correspondence. E-mail tdi@aber.ac.uk; Tel. (+44) (0)1970 622 786; Fax (+44) (0)1970 622 659.

Introduction

Glaciers are increasingly recognized as cryospheric ecosystems, comprising an array of ecological niches and significant microbial populations throughout (Priscu and Christner, 2004; Hodson *et al.*, 2008). Certain microbes tolerate these cold environments well (e.g. Morgan-Kiss *et al.*, 2006; Vincent, 2007) and evidence of interred microbial consortia has been presented for glacier ice of up to 0.75 Ma in age (Abyzov, 1993; Christner *et al.*, 2000; 2003b; Miteva and Brenchley, 2005). Dancer and colleagues (1997) suggested that summer ice ablation will release these microbes to fluvial transport, and Rogers and colleagues (2004) estimated that, globally, 1×10^{17}–1×10^{21} viable microbes could be released annually from glacier melt. With an estimated 2.93×10^6 km^3 of the world's glacier ice in the Greenland Ice Sheet (Bamber *et al.*, 2001) and a further ~ 0.16×10^6 km^3 present elsewhere in Arctic latitudes (Radić and Hock, 2010), the region represents a significant microbial repository. However, regional forecasts of increasing air temperatures and decreasing ice mass (Kattsov *et al.*, 2005; Christensen *et al.*, 2007) indicate consequent effects on ablation and potential microbial mobilization to downstream ecosystems.

Despite a growing interest in the microbial assemblages in glacier habitats (Hodson *et al.*, 2008), few workers have applied flow cytometry (FCM), a tool for microbial enumeration, to glacial samples; existing estimates for cell release by glacier melt have relied on microscopic enumeration or culture of ice cores (see Rogers *et al.*, 2004). FCM has been accepted as a commonplace technique in environmental microbiology for over 25 years (e.g. Yentsch *et al.*, 1983), and has been increasingly applied to freshwater habitats (Collier and Campbell, 1999; Marie *et al.*, 2005; Hammes and Egli, 2010; Wang *et al.*, 2010). Recent examples of the application of FCM

to glacial environments have focused solely on deep ice core samples (e.g. Miteva and Brenchley, 2005; Miteva *et al*., 2009) or microbial concentrations within snowpacks (e.g. Liu *et al*., 2009; Chuvochina *et al*., 2011), rather than supraglacial cell fluxes which may constitute an important addition to labile carbon releases (Hood *et al*., 2009). Consequently, there has been an absence of quantitative observations of microbial transport within glacial streams, and the hydrological processes that transfer them across glacier surfaces, leaving a clear research imperative.

Glacier and ice sheet surfaces characteristically exhibit a now well-known, highly active supraglacial habitat referred to as 'cryoconite', comprising inorganic debris and microbial consortia (Wharton *et al*., 1985; Takeuchi *et al*., 2001b; Säwström *et al*., 2002; Christner *et al*., 2003a; Mueller and Pollard, 2004; Anesio *et al*., 2007; Edwards *et al*., 2011). A key source of the content of cryoconite is thought to be airborne (aeolian) mineral and organic dust, mostly from local rock, talus and moraines, which either deposit attached microbes, or scavenge them from the atmosphere during deposition. Moreover, observations of cryoconite also suggest *in situ* growth (Hodson *et al*., 2010; Langford *et al*., 2010; Takeuchi *et al*., 2010) and redistribution and mixing by meltwater transport (Hodson *et al*., 2007; Mindl *et al*., 2007; Irvine-Fynn *et al*., 2011; Stibal *et al*., 2012). Accordingly, the emphasis given to the enumeration of cells within ice cores disregards processes within supraglacial habitats, and likely misrepresents the true rates of microbe liberation during the summer melt season.

To address this question, we present the first direct quantification of cell transfer through an Arctic supraglacial catchment on Midtre Lovénbreen (hereafter, ML), Svalbard, by using FCM to enumerate biological particles and combining these data with stream-flow gauging to estimate seasonal cell budgets and allied nutrient contributions to run-off.

Results

Primary data

During the ablation season of 2010, a 0.08 km^2 supraglacial catchment on ML remained snow-free (19 July–24 August: Day of Year (DOY)200–236; Fig. 1), and local meteorological observations revealed air temperature (T_a) and incident radiation (IR) were covariant ($r = 0.51$, $P < 0.01$; Fig. 2). Daily glacier ice ablation rates across the catchment averaged 0.014 ($\pm$ 0.0026) m water equivalent (w.e.) over the period of observation; this equated to a total meltwater volume of $\sim 3.6 \times 10^4$ ($\pm$ 15%) m^3 discharged at an average of between 0.009 and 0.013 $m^3\ s^{-1}$ through the catchment outlet named MLSG (Fig. 1). The latter values compare well with the mean observed discharge of 0.021 $m^3\ s^{-1}$ ($\sigma = 0.012$; $n = 32$) given the bias for afternoon (peak melt) evaluations. Observed stream discharge (Q) was not significantly correlated with concurrent T_a ($r = 0.33$, $P = 0.07$) or IR ($r = -0.21$, $P = 0.26$). A brief period of snowfall occurred on DOY227, totalling ~ 25 mm, but within 48 h, the glacier ice surface was again exposed across the catchment.

Extending the methods described by Liu and colleagues (2009), FCM was used to enumerate particles and cells in stream water, surface ice and aeolian particle trap samples (see *Experimental procedures*; Fig. 1). In order to distinguish between biological and non-biological particles, the nucleic acid stain SYBR Green II (Molecular Probes; hereafter, SGII) was added to samples. In all cases, approximately 35% of particles were stained and, therefore, classed as biological, of which ~ 60% were categorized as cells by their geometry, with a modal cell size between ~ 0.1 and 0.5 μm (Table 1). The proportion of particles exhibiting 530 ($\pm$ 15) nm autofluorescence was small, at < 2.5%, and was consistent between the three sample types. Broadly, these similarities suggested that there was little difference in particle characteristics between source, *in situ* and output particle populations.

The mean particle concentration of stream water samples was 1.01×10^5 particles ml^{-1}. Typically, ~ 37% of these particles were classed as biological, of which ~ 53% were cells < 0.5 μm in size (Table 1). The total particulate load was not associated with Q ($r = -0.27$, $P = 0.15$) but showed significant inverse correlation with T_a and IR (respectively, $r = -0.59$ and -0.50, $P < 0.01$). In-stream cell concentrations were also inversely correlated with T_a ($r = -0.52$, $P < 0.01$) but not so with IR ($r = -0.22$, $P = 0.23$). Comparison between the particle enumeration and meteorological data series indicated no clear temporal trends (Fig. 2). The plot of Q against particle concentrations (Fig. 3) showed that concentrations of biological particulates, cells and non-cellular particles all exhibited a strong, non-linear logarithmic relationship with Q ($r^2 > 0.69$). Surprisingly, such a trend was absent for the in-stream inorganic particle loads.

Opportunistic samples collected at 80 m intervals upstream of MLSG on DOY216, 221 and 234 showed no significant systematic relationship between total particle load and elevation – a proxy for contributing area ($0.008 < r < 0.38$, $0.91 > P > 0.19$). However, contrary to the other two sample sets, samples taken on DOY221 indicated a significant increase in cell numbers (for all cell size fractions) with elevation ($r > 0.8$, $P < 0.05$). The opportunistic samples collected from all major supraglacial streams across a transect ~ 180 m above sea level (Fig. 1) suggested that catchments contacting ice-marginal sediments carried enhanced concentrations of all particles: total particle concentrations were between 119% and 268% of those in the MLSG catchment, where

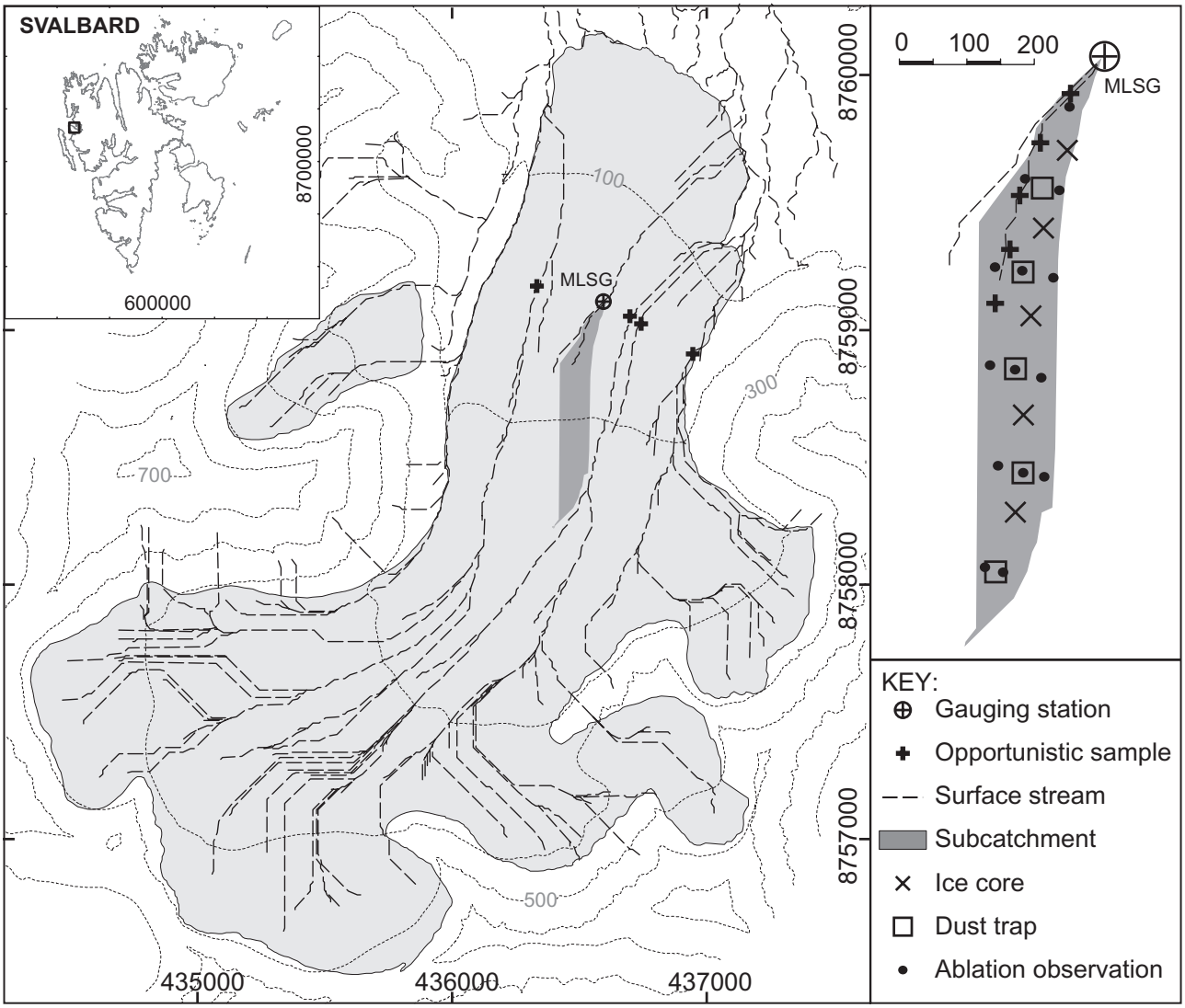

Fig. 1. Location map of ML, in UTM projection, illustrating ice extent, key supraglacial drainage pathways and sampling locations. Contours at 100 m intervals are indicated with dotted lines. The accompanying panel details the positions of sample points, shallow ice core extraction, and aeolian particle (dust) trap location within the supraglacial catchment.

no moraine is present. Importantly, the relative proportions of biological particles and cells remained equitable to those found in the MLSG samples (33–43% and 54–64% respectively; cf. Table 1). The distribution of relative fractions of cell sizes were also similar between supraglacial streams, but with a slightly reduced number of large (> 3.0 μm) cells in MLSG waters.

The mean concentrations of 2.67×10^5 total particles ml^{-1} and 5.70×10^4 cells ml^{-1} in the ice core samples were approximately three times greater than in stream waters. Nonetheless, as found in the stream samples, ~ 35% of particles were biological, of which ~ 60% were classed as cells; in both instances, this was shown to be statistically similar ($|t| < 1$, $P > 0.05$). However, in contrast to the stream samples, there was greater variability in the relative proportions of the < 0.5 μm and 0.9–3.0 μm size fractions (Table 1). Using Kruskal–Wallis and Welch tests, appropriate for the data set, no significant difference existed between the distributions, medians and means of the concentrations of total particulates and biological particles, and cells in each size fraction for sequential 25 cm depths of the 1 m surface ice cores ($P > 0.26$, for all cases). Conversely, comparison of the averages and distributions of particle concentrations between the five shallow ice cores were significantly different for all categories ($P < 0.04$) with exception to cells < 0.5 μm ($P > 0.61$). The three lowermost cores exhibited the most similarity, while data from the core taken from ~ 230 m above sea level (a.s.l.) indicated enriched particle concentrations at all depths (Fig. 4). The relative proportion of

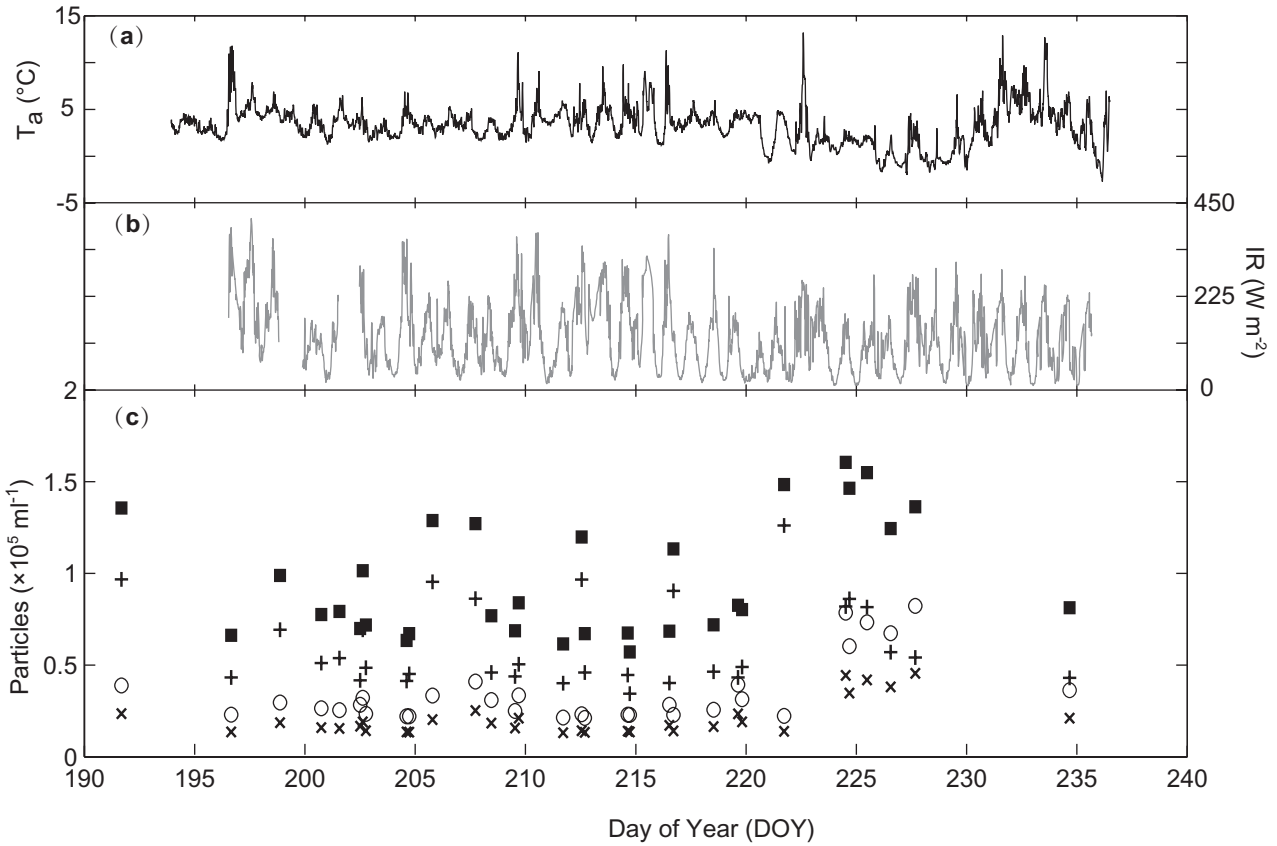

Fig. 2. Time series of (a) air temperature (T_a); (b) incident radiation (IR); and (c) particle concentrations: total (filled squares), inorganic particles (+), biological particles (hollow circles) and cells (×).

autofluorescent particles was equivalent to that observed in the stream samples.

For data derived from the aeolian particle traps, with the exception of the proportion of larger (0.9–3.0 μm) cells, the distribution of classified populations was statistically different to that of the in-stream samples ($|t| > 2.0$, $P < 0.05$). Specifically, there appeared to be an increase in the proportion of biological particles by ~ 20% with a more equitable distribution of cells across the size ranges (Table 1). Compared with stream and ice core samples, a small quantity of aeolian particles exhibited autofluorescence (~ 1%). Interestingly, compared with the single snow sample, a greater portion of the aeolian particles were biological, while the snow sample evidenced a

Table 1. Summary of FCM particle enumeration for the four differing sample sources: meltwater, ice, aeolian particle traps (corrected for UFDI inclusions) and snow (collected during snowfall event on DOY227).

	Stream MLSG		Ice core		Aeolian traps		Snow	
Samples (*n*)	37		20		21		1	
Quantity	μ	σ	μ	σ	μ	σ		Units
Total (× 10^5)	1.01	0.49	2.98	2.94	0.07	0.06	0.83	per ml
AF particles	1.6	0.8	*1.3*	*0.5*	*1.0*	*0.6*	2.4	% total
SGII stained	36.7	10.6	35.2	9.2	55.6	22.4	28.4	% total
Cells	59.9	2.0	61.4	3.8	64.2	6.7	59.3	% SGII stained
Cells ≤ 0.5 μm	53.8	5.3	44.9	12.7	38.8	25.9	52.6	% cells
Cells ≤ 0.9 μm	19.5	1.6	19.4	1.5	26.4	11.1	17.7	% cells
Cells ≤ 3.0 μm	26.7	4.7	33.7	10.6	26.3	11.0	29.2	% cells
Cells > 3.0 μm	0.6	0.5	2.0	1.3	9.1	13.5	0.4	% cells

The number of samples (*n*) is shown and data reported as means (μ) and standard deviations (σ). For each cell size fraction, '≤ 0.9 mm' is defined as '0.5 mm < cell ≤ 0.9 mm'.
Autofluorescent (AF) particles were determined from unstained samples; instances where a subsample was used for enumeration are *italicized*.

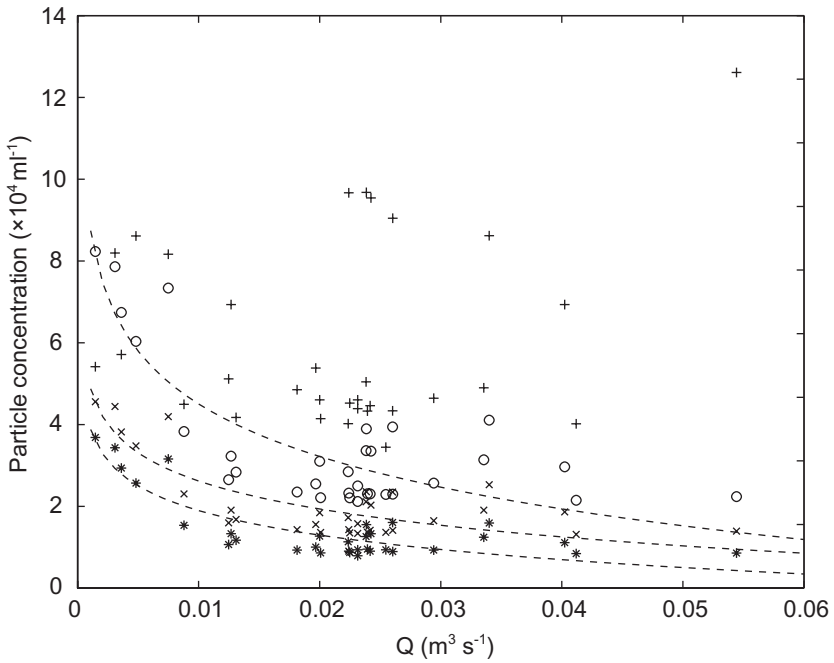

Fig. 3. Plot of discharge (Q) against particle concentration for inorganic particles (+), biological particles (hollow circles), cells (×) and residual biological fraction (*). The logarithmic trend lines ($r^2 > 0.69$) for the latter three categories are indicated.

greater proportion of autofluorescent particles (2.4%). Over the period of observation, accounting for the supraglacial catchment area, a total quantity ~ 9.5×10^{15} particles or ~ 6.1×10^{15} cells may have been delivered to the ice surface (see *Experimental procedures* for details). No systematic temporal trends in delivery of particles or cells were found for individual traps or trap application periods.

Particle budgets

The fluvial export of particles (or cells) from the glacier surface (P_f) for a given period of time is likely to reflect a simple budget equation:

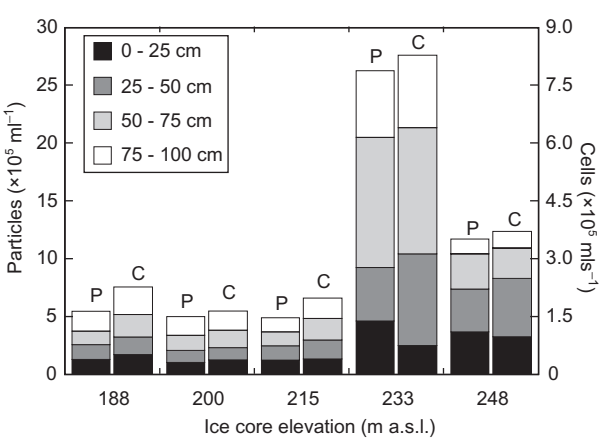

Fig. 4. Illustration of particle (P) and cell (C) distribution over depth in near-surface ice core samples.

$$P_f \pm \Delta S = P_a + P_i \quad (1)$$

for which, respectively, P_a and P_i represent the number of particles (or cells) derived from aeolian sources and the glacier ice melt; the term ΔS represents a storage component involving physical transport processes and biologically mediated changes at the ice surface. For each trap installation period, aeolian particle fluxes across the supraglacial catchment averaged 1.37×10^8 particles m^{-2} h^{-1} which included 4.69×10^7 cells m^{-2} h^{-1}. Note that, in the absence of fully detailed glacier surface boundary layer data (e.g. wind velocity profiles etc.), accurate particulate deposition rates or quantities are incalculable. The flux of particles sourced from ice melt (P_i) was estimated on the basis of average surface ice core concentrations and the ablation records, yielding values of 1.56×10^8 particles m^{-2} h^{-1} and 5.22×10^7 cells m^{-2} h^{-1}. Sampling of ice cores at the close of the season ensured samples would not be affected by refrozen ice associated with seasonal snowmelt.

To provide an estimation of cell numbers discharged through MLSG as the ablation season progressed, we adopt the method described by Tranter and colleagues (2002) for calculating nutrient fluxes: representative concentrations of cells are derived from the linear regression between Q and cell flux (Fig. 5). Details of the regression relationships between Q and microbial populations discriminated by size are shown in Table 2. Using the estimated mean discharge of 0.012 m^3 s^{-1}, the total numbers of biological particles and cells liberated from the supraglacial catchment's surface over the observation

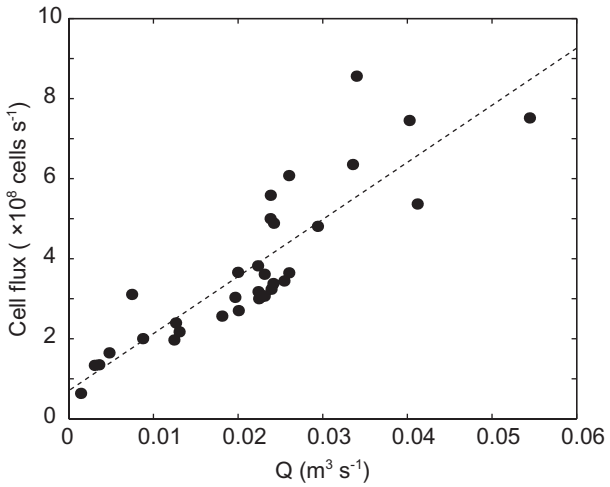

Fig. 5. Regression to derive representative concentrations of cells.

period are 1.26×10^{15} and 0.75×10^{15} respectively. These equate to approximate fluxes (P_l) of 4.20×10^7 particles $m^{-2}\,h^{-1}$ and 1.08×10^7 cells $m^{-2}\,h^{-1}$. Balancing Eq. 1 for the MLSG catchment, ΔS for particles and cells is positive ($+2.51 \times 10^8$ particles $m^{-2}\,h^{-1}$ and $+8.83 \times 10^7$ cells $m^{-2}\,h^{-1}$ respectively) highlighting inefficient transport at the ice surface and net storage of particles and cells. This may be further compounded by growth *in situ* (Anesio *et al*., 2010). Crucially, the ratio of stream to ice core sample particle concentrations was shown to be 0.33–0.35, and the total and the number of cells transported by the supraglacial stream over the period of observation (7.51×10^{14} cells) was 37% less than the potential cell numbers sourced in the glacier ice alone (2.01×10^{15} cells).

Discussion

Particle enumerations

The mean stream water concentrations of $\sim 3 \times 10^4$ biological particles ml^{-1} and $\sim 2 \times 10^4$ cells ml^{-1} corresponds to published values for bacteria and/or cell abundance in glacial meltwaters at ML (Anesio *et al*., 2007; Mindl *et al*., 2007; Rassner, 2009); the range of ice core cell concentrations found in the MLSG catchment of 1.83×10^4–2.25×10^5 cells ml^{-1} lie well within published in-ice concentrations ranging from 7.0×10^2 to 1.4×10^7 cells ml^{-1} (Miteva and Brenchley, 2005; Price *et al*., 2009). The proportion of cells within the aeolian samples was broadly similar to those in ice and stream samples, a finding reiterated by Segawa and colleagues (2005) who reported the delivery and elution of microbes from a mountain snowpack, and Hawes's (2008) indication that the southerly winds, which characterize the ML catchment, deliver organic material to the local terrain surface.

Critically, FCM indicated a large proportion of cells identified here were < 0.5 μm. This value is in agreement with previous glacial studies reporting microbial dimensions (e.g. Sheridan *et al*., 2003; Miteva and Brenchley, 2005; Mader *et al*., 2006; Tung *et al*., 2006). In this instance, without information about these cells' phylogenetic affiliation, it is unclear whether they represent cells with a stable phenotype of small cell size, or diminutive 'dwarf' incurred by nutrient limitation and other stresses likely at the glacier surface (Miteva and Brenchley, 2005). Rogers and colleagues' (2004) estimate of up to 1×10^{21} microbes liberated annually from glacier ice referred to viable microorganisms. Here, FCM was not used to explore cell viability, although previous FCM research has suggested the potential for assessing this quantity (Boulos *et al*., 1999). Nonetheless, the ambiguity of 'cell viability' remains problematic in dual-staining analyses (Berney *et al*., 2007), especially in light of recent experimental assessments illustrating that viable cells can absorb supposedly 'nonviable' stains in response to physical or chemical stresses (e.g. Phe *et al*., 2007; Davey and Hexley, 2011). Failure to achieve dual-staining of cryoconite samples has been found previously (M. Stibal, pers. comm., 2010), which may suggest that microbes on glacier surfaces may be close to stress thresholds, as supported by the cell dimensions reported here. Assessment and quantification of viable cells from the supraglacial ecosystem, therefore, remains undetermined.

Interestingly, the enumeration showed that in-stream autofluorescent particles, of which 60.8% were geometrically similar to microbial cells, displayed statistically sig-

Table 2. Representative particle and cell concentrations (equivalent to the slope) as derived from the regressions of Q vs. cell flux, the standard error (SE) of the slopes, the regression intercepts (constant) and the coefficients of determination (r^2).

	Biological particles	All cells	Cells ≤ 0.5 μm	Cells ≤ 0.9 μm	Cells ≤ 3 μm	Cells > 3 μm	Inorganic particles
Slope ($\times 10^9$)	22.6	14.3	6.77	3.02	4.43	0.09	86.6
SE ($\times 10^8$)	24.9	14.9	9.10	3.23	4.03	0.30	114
Constant ($\times 10^7$)	13.5	7.03	5.11	0.91	1.08	–0.02	–51
r^2	0.73	0.75	0.65	0.74	0.80	0.25	0.65

Cells for each sequential size fraction are indicated, for example, '≤ 0.9 μm' relates to the window defined as 0.5 μm < cell ≤ 0.9 μm.

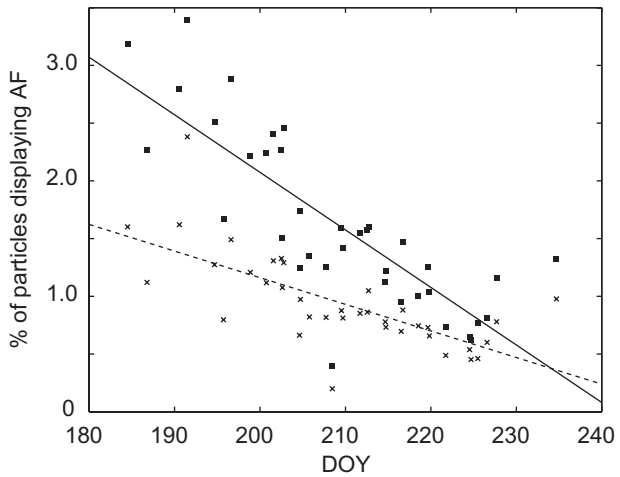

Fig. 6. Time series of in-stream autofluorescent particles (filled squares) and cells (×) over the period of observation.

nificant temporal trends at the $P = 0.01$ level (for particles, $r = 0.66$; for cells, $r = 0.49$; Fig. 6). The likelihood of this observation being the result of sample-run contamination was discounted as repeat blank samples included intermittently in the analytical run yielded outlying results independent from the trend. In analyses of microbes within ice, the presence of a blue-excitation green-autofluorescent subpopulation, typically < 3% of the total population, has been associated with methanogens (Tung *et al*., 2005; Price, 2007) exhibiting coenzyme F_{420} which was thought a specific biomarker of methanogenic archaea (DiMarco *et al*., 1990). However, this diagnostic is equivocal (Purwantini *et al*., 1997; Boyd *et al*., 2010). Indeed, F_{420} can be present in many actinobacteria, members of which are represented in clone libraries of ML cryoconite (Edwards *et al*., 2011). In certain actinobacteria, changes in autofluorescence are ascribed to the concentration and oxidation status of flavins such as F_{420} and pyridines in relation to metabolic status; thus it is possible the seasonal change in autofluorescent cell counts relates to changes in cell activity and viability (Kell *et al*., 1991).

The observed ablation of 0.44 m w.e. across the MLSG catchment during 2010 broadly agrees with estimates for typical specific glacier ice melt at ML of 0.27 ± 0.15 m (Hodson *et al*., 2005). However, the disparity implies some of the observed ice melt may have included refrozen snowmelt or superimposed ice, which is common on ML (Wadham and Nuttall, 2002). Consequently, the seasonal decrease of the autofluorescent population may relate to the release of microbes from superimposed ice, which progressively decreased as ablation continued. This is further supported by the results from the snow sample which indicated the greatest proportion of autofluorescent particles. However, the identity of the autofluorescent subpopulation remains unknown.

Implied hydraulics and characteristics of the supraglacial habitat

The apparent storage of cells and particles revealed in this study implies existing global estimates of cell liberation from ice masses based on ice core data may misrepresent the contemporary microbial delivery to downstream environments, in part due to complexity in surface ice hydraulics. Consequently, the mechanism(s) by which particles may be retained at the glacier surface demands further consideration. The melting surface of a glacier consists of a shallow (< 2 m) layer of reduced density, porous ice termed the 'weathering crust' (Müller and Keeler, 1969); however, the hydraulic characteristics of this weathering crust remain poorly understood (e.g. Munro, 2011). Nonetheless, the results presented here provide insight into the hydraulic conditions of this shallow surface ice layer and a number of the complexities.

First, the mean ice core cell concentration of 5.70×10^4 cells ml^{-1} exceeds the asymptotic concentration of $\sim 0.84 \times 10^4$ cells ml^{-1} seen in the stream for $Q > 0.05$ m^3 s^{-1} (Fig. 3). If efficient particle transport through ice ablation occurred, ice core concentration would be likely to equal in-stream concentrations at high Q, as the process of concentration dilution would be offset by the particle inclusions within the melting ice. The analysis of the near-surface ice cores showed there was no increase in particle or cells concentration with depth, negating gravity-driven particle accumulation at the base of the weathering crust, which rarely exceeds 1 m in depth in central–western Svalbard (Sobota, 2009). Moreover, the absence of a discharge – particle concentration relationship for the inorganic particles, suggests that, by inference, the mineral load was potentially influenced by stochastic processes of input or entrainment, perhaps including the disaggregation of 'cryoconite granules' which exhibit biota only at the outmost edges (Hodson *et al*., 2010). These findings contrast to those presented in Segawa and colleagues (2005) who suggested equivalence between mineral and organic particles drained from a mountain snowpack. Thus, the delivery of particles to supraglacial streams is mediated by processes on and within both cryoconite and the weathering crust.

Second, the observation that, statistically, the relative proportions of cells and cell sizes varied between aeolian particles (input), the ice core (throughput) and in-stream samples (output) suggests that the weathering crust may act as a filter. This latter notion is perhaps exemplified in the non-linear relationship between Q and biological particle concentrations: at low Q, which by definition will be when ice melt rates are also reduced, the elevated concentrations of particles suggests effective transport through the weathering crust. However, as Q increases, three concomitant processes may explain the variation in

particle transport: first, analogous to englacial hydraulics (e.g. Röthlisberger, 1972), as Q rises, at the local scale, larger interstitial flow paths may effectively capture and reduce water flow from other portions of the weathering crust thereby decreasing the areas contributing to cell entrainment. Second, analogous to subglacial hydrology (e.g. Hubbard *et al*., 1995), at times of increased melt, the weathering crust becomes waterlogged, with water pressures directing flow away from preferential flow paths, and reducing contributions from interstitial spaces; at low melt, the pressure gradient is reversed and potentially enhancing apparent particle transport through the porous media. Third, the particles themselves may impede transport rates and clog interstitial spaces within the weathering crust (cf. Mader *et al*., 2006), thereby reducing the numbers and geometries of particles liberated into stream waters and represented in the disparity between particle size distribution (see Table 1). Here, we note that we are unable to quantify either biological cell proliferation or physical degradation, which may also contribute to determining the hydraulic properties of the weathering crust as well as the variations in cell numbers and size distributions between input, throughput and output locations.

Finally, the implications of particle, cell and carbon accumulation within glacier near-surfaces, as demonstrated here, has a significant glaciological component. The presence of particles and biological activity on glacier ice markedly reduces the ice reflectivity or albedo (Takeuchi, 2002). An active microbial community, through the production of humic substances and pigments or the amalgamation of particles by biofilm formation, can then further reduce the glacier ice albedo (Kohshima *et al*., 1993; Takeuchi *et al*., 2001a; Hodson *et al*., 2010). This process increases the shortwave radiation available for ice melt and so is becoming an important area of research for glacier surface energy balance (e.g. Takeuchi, 2009; Bøggild *et al*., 2010; Irvine-Fynn *et al*., 2011). Critically, the potential decadal longevity of cryoconite on glacier surfaces has previously been demonstrated using geochemistry (Tieber *et al*., 2009), thin section microscopy (Takeuchi *et al*., 2010) and time-lapse imagery (Irvine-Fynn *et al*., 2011). Consequently, a net gain of particulates within and at an ice surface may cause an apparent darkening, reducing the albedo, and enhancing the melt rate on decadal timescales. If the single season of observations on ML is representative of a supraglacial process, the accelerating rate of ice mass thinning reported for the glacier (Kohler *et al*., 2007) may have a biological component to its cause, not solely climate forcing.

Implications for supraglacial nutrient export

Although the overarching finding here is the accumulation of particles at an Arctic glacier surface, a proportion was released to aquatic and downstream environments. As other researchers have done in differing contexts (e.g. Anesio *et al*., 2009; Boyd *et al*., 2010), it is tempting to use Table 2 to upscale results to estimate cell delivery to downstream environments at the global scale. However, the unverified representativeness of site-specific studies as analogues for global ice masses suggests such extrapolations should be treated with caution. Nonetheless, supraglacial drainage on ML is dominant (Hodson *et al*., 2005; Irvine-Fynn, 2008): ~ 71% of the glacier's surface area drains supraglacially and 70% of the glacier area is below the long-term average equilibrium line altitude (ELA) of 400 m a.s.l.; consequently, we upscale our estimates to the glacier scale. Assuming the 0.44 m w.e. ablation is representative for the ablation area of the glacier, a total of 2.37×10^{16} cells were released into the proglacial environment over the 36 day, snow-free observation period. Since across-glacier assessment of in-stream particle concentrations showed significant increases where contributing meltwaters contacted ice-marginal areas, this latter estimate must be considered a minimum.

The export of cells from glaciers has potential impacts upon downstream ecosystems; the data available here permit an estimation of seasonal carbon, macronutrients and macromolecules. Conversion from cell numbers to carbon content was based on a factor of 20 fg C $cell^{-1}$ as previously used to estimate aquatic prokaryotic cellular carbon (Whitman *et al*., 1998). Separately, assuming a median particle size for each subpopulation, and assuming cells to have a near-spherical form (see *Supplementary information*, Fig. S1c), total biovolumes of each of the size fractions and hence cellular carbon content could be calculated from the FCM data using the allometric relation between cell size carbon applied to FCM enumerated cells from freshwater by Felip and colleagues (2007). Using the relationships detailed in Table 2 for each size fraction, over the 36 day period of observation, and given the rapid supraglacial run-off velocities at ML of the order of 0.5 ms^{-1} (Irvine-Fynn *et al*., 2005) and lengthy biomass doubling times in meltwater ~ 8 days, according to Anesio *et al*., (2010), estimates of the released mass of macronutrient and macromolecule can be made not only for MLSG but also for the typical ablation area on ML (Table 3). A total of 15.1–72.7 g C as particulate organic carbon (POC) is delivered to downstream locations by cells from the MLSG catchment, and 0.48–2.7 kg C was released from the glacier's surface which may represent an important addition to dissolved organic carbon (DOC) which is also known to be sourced on glacier surfaces (e.g. Barker *et al*., 2006; Hood *et al*., 2009). Note that the estimates of nutrient release presented here are minima since they ignore contributions from the residual biological fraction identified in the FCM analyses.

Table 3. Estimation of annual cellular carbon, macronutrient and macromolecule fluxes from the MLSG catchment and for ML, in g and kg, respectively. Calculations assume either a constant 20 fg C per cell[a] or allometric C-per-cell[b], and published ratios (and uncertainties) of carbon to constituents.[a,c–f]

	MLSG (g a^{-1})		ML (kg a^{-1})	
Nutrient	Constant	Allometric	Constant	Allometric
Carbon	15.1	72.7	0.48	2.69
Nitrogen[c,d,e]	3.2 (± 0.7)	15.3 (± 3.4)	0.10 (± 0.02)	0.56 (± 0.13)
Oxygen[c,e]	5.6 (± 2.4)	26.9 (± 11.7)	0.18 (± 0.08)	0.99 (± 0.43)
Phosphorus[c]	0.9 (± 0.3)	4.4 (± 1.3)	0.03 (± 0.01)	0.16 (± 0.05)
Sulfur[c]	0.5 (± 0.3)	2.2 (± 1.5)	0.01 (± 0.01)	0.08 (± 0.06)
DNA[f]	2.4 (± 0.7)	11.6 (± 3.6)	0.08 (± 0.02)	0.43 (± 0.13)
RNA[f]	2.7 (± 0.0)	13.2 (± 0.2)	0.09 (± 0.0)	0.49 (± 0.01)
Protein[f]	17.4 (± 0.2)	83.9 (± 0.8)	0.55 (± 0.01)	3.11 (± 0.03)

a. Whitman and colleagues (1998).
b. Felip and colleagues (2007).
c. Fagerbakke and colleagues (1996).
d. Fukuda and colleagues (1998).
e. Vrede and colleagues (2002).
f. Simon and Azam (1989).

Such estimates can also be extended to cellular nitrogen, oxygen, phosphorus, sulfur, DNA, RNA and protein (Table 3), based on averaged stoichiometric carbon-to-compound ratios reported for aquatic bacteria (Simon and Azam, 1989; Fagerbakke *et al.*, 1996; Fukuda *et al.*, 1998; Vrede *et al.*, 2002). These data suggest 0.10–0.56 kg of nitrogen and 0.55–3.1 kg protein was liberated from the glacier surface and transferred to the forefield and beyond during the observation period. Of particular interest, however, is the genetic potential arising from the 0.08 kg a^{-1} to the 0.43 kg a^{-1} flux of cellular DNA from ML. From the data in this study the actual genetic influence cannot be inferred, although analyses of bacterial 16S ribosomal RNA genes reveal remarkably high bacterial diversity in supraglacial melt streams (including from MLSG) on ML relative to freshwater habitats in its forefield and tundra lakes (Rassner, 2009) thus underlining the potential for gene flow from the supraglacial ecosystem in specific circumstances.

Concluding comments

This study has provided the first quantification of particle and cell budgets for a high-Arctic glacier surface, estimating POC and nutrient export from the ice surface, and demonstrating the potential for particle retention within the weathering crust during summer months. Extending this to the cryosphere more generally, when coupled with the potential for supraglacial carbon fixation (Anesio *et al.*, 2009), the physical retention of particulates at glacier surfaces, while permitting supraglacial sequestration of carbon, may be contributing to the thinning of and decline in ice mass volumes through the feedbacks altering ice albedo. This has mounting credence following suggestions that there have been increases in global atmospheric dust, aeolian dust deposition and aquatic environment productivity over the last century (e.g. Mahowald *et al.*, 2010). Although, in specific circumstances, substantial volumes of cells, genes and nutrients may be exported fluvially, due to the net retention of particles in the surface ice matrix, the down-wasting of glacier ice masses may also directly 'seed' the newly exposed terrain at retreating glacier margins. However, the particle fluxes and storage reported here will have inter-annual variability, and we hypothesize that, over the medium-term, seasonal snowmelt sources and summer season precipitation events may play a role in delivering, modulating or flushing particulates within and from the weathering crust. Accordingly, to confirm such assertions, and to ascertain if the 'biological darkening' of glaciers is a worldwide or persistent phenomenon, longer-term monitoring of particle and cell fluxes to, through and from glacier surfaces is needed.

Experimental procedures

Study site

Midtre Lovénbreen is a 5 km^2 valley glacier in north-west Svalbard (78°53′N, 12°05′E) and ranges from 50 to 650 m a.s.l. (Fig. 1). As one of the most studied glaciers in the high-Arctic, its glaciology is well described (e.g. Björnsson *et al.*, 1996; Hambrey *et al.*, 2005). Recently, the glacier has been a focus for microbiological study, both subglacially (e.g. Wynn *et al.*, 2007; Irvine-Fynn and Hodson, 2010) and supraglacially (e.g. Hodson *et al.*, 2007; Mindl *et al.*, 2007; Telling *et al.*, 2010; Edwards *et al.*, 2011). Hodson and colleagues (2007) estimated that 1% of ML's supraglacial environment is covered by cryoconite deposits. A supraglacial catchment drained by a single stream with no moraine outcrops, ice-marginal zones or hydrological features draining to englacial locations was loosely defined using an ArcGIS-based hydro-

logical analysis of a digital elevation model of ML derived from airborne laser profiling in 2005 (see Barrand *et al*., 2010; Fig. 1). The gently sloping catchment, ranging from ~ 175 to 270 m a.s.l. with a mean surface slope of 9.9 (± 2.1)%, was assumed constant over the study period.

Field data

Stream discharge (Q) with an maximum uncertainty of ± 10% was gauged using saline and Rhodamine WT dilution techniques (Keller, 1969; Day, 1976). Key meteorological data of air temperature (T_a), incident shortwave radiation (IR) and wind speed (u) were also recorded at hourly intervals at MLSG during the period of observation, with respective uncertainties of ± 0.1°C, ± 10%, and ± 0.2 m s^{-1}.

Discrete ice ablation observations, to an accuracy of ± 5 mm, were observed periodically across the catchment at ~ 4 day intervals using 12 reference stakes secured into the glacier ice (see Müller and Keeler, 1969; Fig. 1). Specific ablation was expressed in metres water equivalent (m w.e.) assuming the standard glacier ice density value of 900 kg m^{-3} (e.g. Konzelmann and Braithwaite, 1995).

Stream and ice core sampling

Coincident with stream discharge records at MLSG, 40 ml samples of supraglacial water (at ~ 0.1°C) were collected periodically using sterile 50 ml centrifuge tubes that were thrice-rinsed with > 30 ml of stream water before sampling. Opportunistic samples were also collected from streams both across- and up-glacier; such sample sets were collected within a 30 min time window for comparison. Samples were stored within 8 h of collection at −80°C and not chemically fixed prior to analysis. This protocol minimized potential effects on in-sample particulates and precipitation of formaldehyde solutions (necessary for chemical fixation) for microbial analysis of non-preserved, low temperature aquatic samples (Walker, 1931; Turley and Hughes, 1992; Trousselier *et al*., 1995; Kamiya *et al*., 2007). The method is assumed robust (see Mader *et al*., 2006).

At the end of the observation period and across over the catchment elevation range (Fig. 1), five cores of surface glacier ice were drilled with a Kovacs Mk II coring system to depth of 1 (± 0.03) m and separated into 0.25 (± 0.02) m sections. The 1 m depth corresponds to the locality's seasonal development of the weathering crust (Sobota, 2009). The corer was sterilized with ethanol and a pilot test core was drilled to 'rinse' the corer barrel; core-hole water was used to rinse the barrel prior to each subsequent sample. The ice cores were handled with sterile nitrile gloves to prevent latex contamination, placed on clean polypropylene tubing, and divided using cleaned stainless steel blades. Ice core sections were placed in individual, sterile sample bags, allowed to thaw completely at ~ 4°C, and then agitated: 40 ml of sample was extracted with a sterile syringe and stored at −80°C.

Aeolian particle samples

To measure vertical, wet and dry aeolian particle fluxes, five traps were installed along the supraglacial catchment's centre line (Fig. 1). The traps followed the inverted Frisbee design (Hall and Waters, 1986; Goossens, 2005): secured to a dark, narrow 500 ml sample bottle, the Frisbee was lined with clean aluminium foil and filled with 1.25 cm diameter glass marbles. The marbles provided a macro-roughness mirroring that of ablating ice surface, yet have negative zeta potential (Salerno *et al*., 2004) promoting electrical stability and low micro-roughness to discourage splash-out by precipitation and encourage effective rinsing of cells into the bottle (Shellenbergen and Logan, 2002). Prior to each application of the aeolian particle traps, the marbles were rinsed six times in ultrafiltered (0.1 μm) deionized water (hereafter, UFDI) and remained on sterile aluminium trays at 140°C for 3 h. The traps and any liquid precipitation were collected at 7–10 day intervals in sterile sample bags, totalling five times over the study period. For each collection, the foil and marbles were washed with a known volume of UFDI water, which was subsequently sampled and stored at −80°C. Background particulate content was estimated from UFDI water taken as sample blanks. Nitrile gloves were worn for handling of the aeolian particle traps and samples.

Flow cytometry

All samples were thawed at ~ 4°C and immediately analysed with a BD Biosciences LSR-II flow cytometer. The biological component of the particulate loads was stained with SGII, which markedly increases the green fluorescence (530 nm) of particles containing nucleic acids excited by a 488 nm (blue) argon ion laser; SG II is considered the most appropriate stain for differentiating and enumerating microbes in freshwater samples (Lebaron *et al*., 1998; Weinbauer *et al*., 1998). Following Lebaron and colleagues (1998), 2 μl of 1:10 000 SYBR Green II stock solution was diluted in 1 ml Phosphate Buffered Saline (pH 7.4), from which 1 μl was added to 2 ml of sample in a sterile vial and incubated for 30 min in the dark at ~ 23°C prior to FCM analysis.

Comparison of analyses with stained and unstained samples permitted the setting of a green fluorescence threshold (or gate) to discriminate biological from mineral particles which exhibited only very weak signal on the 530 nm detector (see *Supplementary information*, Fig. S1). In subsequent runs of unstained samples, particles that yielded a green signal were classed as autofluorescent. A run of trial samples, stained with SGII, showed two clear populations on plots of forward against side scatter (respectively, FSC and SSC, which are geometric descriptors of particles): a large region of scatter broadly showing a highly correlated relationship between the two variables, and a population with low FSC, but a range of SSC (Fig. S1c). The former population was taken to reflect a cell population. The latter, here classed as 'residual biological fraction', was suggestive of a particulate population comprising fragmented or degraded cells or nucleic acids (DNA/RNA), or viral particles. Support for this interpretation is given by virus geometries and fluorescence signals (Brussaard *et al*., 2000), supraglacial viral abundance observed proximate to MLSG (Rassner, 2009) and potential fluorescent 'noise' associated with organic, non-cellular particulates and aerosols found within glacier ice (Price *et al*., 2009). Setting gates to define cells, these were then differentiated by size: size categories were defined using 0.5, 0.9

Table 4. Details of uncertainty in enumeration values given as percent relative standard deviation (%RSD) derived from *n* replicate samples and/or deionized water pseudo-blanks.

	Samples (*n*)	All particles	Biological particles	Cells (all)	Cells < 0.5 μm	Cells < 0.9 μm	Cells < 3.0 μm
Stream MLSG	11	0.3–4.1	1.4–5.1	1.3–5.9	1.3–4.1	1.4–8.9	2.6–9.9
Ice core	5	0.9	2.8	3.2	3.2	5.2	3.1
Aeolian particle traps	5	2.1	6.8	6.4	7.1	6.8	3.9

Stream samples comprised multiple analytical runs resulting in a range of potential errors.

and 3 μm Megamix (BioCytex, France) fluorescent beads (Fig. S1c). Because FSC is highly sensitive to particle geometry and alignment, SSC provides the more reliable measure of 'size', although synthetic beads may have increased fluorescence compared with natural particulates (Nebe-von-Caron, 2009); consequently, the four size fractions reported here are approximate not absolute.

Flow cytometry analysis using FACSDIVA 6.1.1 software enumerated all particles in each experimental gate: (i) all particles, (ii) stained biological particles, (iii) cells and (iv) cell numbers in each size fraction (< 0.5 μm, 0.5–0.9 μm, 0.9–3.0 μm and > 3.0 μm). Numbers of particles assumed to be inorganic or classed as residual biology were calculated by subtraction. The precision of enumeration was evaluated as percentage relative standard deviation (%RSD) derived from replicate samples included within each analytical run (Table 4): measurement uncertainties were < 10%.

Previous research has argued that, particularly for sediment-rich samples, enumerations for quantifying cell abundance using nucleic acid stains may be erroneous due to intrinsic autofluorescence, noted for some metal oxides and non-specific binding to mineral and (organo-)clay particles (e.g. Klauth *et al*., 2004; Morono *et al*., 2009). Non-specific staining of particles by SGII exhibits a Stokes shift in blue-stimulated, peak green fluorescence to ~ 560 nm (Sunamura *et al*., 2003; Klauth *et al*., 2004). For manual or image-based microscopy, the presence of stained mineral and autofluorescent particles may manifest itself as overestimation of biological particles, while in the presence of organo-clays, the Stokes shift may mask microbial signatures. Here, using FCM, uncertainties are reduced by the use of the narrow 530 ± 15 nm detector bandwidth.

Aeolian particle trap data

Nearly all aeolian particle traps have limited efficiency (Sow *et al*., 2006) and UFDI is not necessarily particle free (Wang *et al*., 2007). Therefore, data drawn from the aeolian particle traps demanded correction. First, the FCM enumerations were corrected by subtracting the background particle concentration derived from the analysis of the UFDI water used for each trap application. Laboratory incubations of revived glacial community samples indicate population numbers remain relatively stable for 3–10 days (H. Langford, unpubl. data; also cf. Anesio *et al*., 2010); when coupled with the dry storage of trap-captured particulates, this suggests that post-depositional growth can be presumed negligible for the trap installation periods. Accounting for the 'wash water' volume and duration of each trap instalment (t_i), the aeolian particle flux (P_a) could be calculated as:

$$P_a = (cV)/(A_f E t_i) \tag{2}$$

where c is the concentration of particles derived from the FCM analysis, V is the volume of wash fluid, A_f is the Frisbee area (here, 0.0397 m^2) and E the aeolian particle trap efficiency correction factor derived by Sow and colleagues (2006):

$$E = k_1u^6 + k_2u^5 + k_3u^4 + k_4u^5 + k_5u^2 + k_6u + k_7 \tag{3}$$

for which, for particles < 19 μm in diameter, the constants $k_{1\Rightarrow7}$ are empirically derived and assumes negligible differences in Frisbee aerodynamics (see Hall and Waters, 1986). The variable u is the estimated boundary layer wind speed calculated from the recorded meteorological data.

Acknowledgements

All authors acknowledge NERC Standard Grants NE/G00496X/1 and NE/G006253/1 (to AMA and AJH). TI-F and AE recognize support from the Climate Change Consortium of Wales (C3W) initiative and Aberystwyth University Research Fund respectively, facilitating completion of the manuscript. Logistical support from the NERC Arctic Research Station (Ny-Ålesund) through Nick Cox, and the field assistance from Jon Bridge, Jon 'Hawkeye' Hawkings, Guy Hillyard, Aga Nowak and other Harland Huset inmates was gratefully received. Kay Hopkinson aided in the FCM analyses. We thank Hazel Davey, Gareth Griffith, Bryn Hubbard, and Nozomu Takeuchi for their reading of and insightful commentary on the manuscript. Comments from anonymous reviewers were highly valuable in realizing this final version.

References

Abyzov, S.S. (1993) Microorganisms in the Antarctic ice. In *Antarctic Microbiology*. Friedmann, E.I. (ed.). New York, USA: Wiley-Liss, pp. 265–295.

Anesio, A., Mindl, B., Laybourn-Parry, J., Hodson, A., and Sattler, B. (2007) Viral dynamics in cryoconite holes on a high Arctic glacier (Svalbard). *J Geophys Res* **112** (G04S31). doi:10.1029/2006JG000350

Anesio, A.M., Hodson, A.J., Fritz, A., Psenner, R., and Sattler, B. (2009) High microbial activity on glaciers: importance to the global carbon cycle. *Global Change Biol* **15:** 955–960.

Anesio, A.M., Sattler, B., Foreman, C., Telling, J., Hodson, A., Tranter, M., and Psenner, R. (2010) Carbon fluxes through bacterial communities on glacier surfaces. *Ann Glaciol* **51:** 32–40.

Bamber, J.L., Layberry, R.L., and Gogineni, S.P. (2001) A new ice thickness and bed data set for the Greenland Ice Sheet 1 – measurement, data reduction, and error. *J Geophys Res* **106** (D24): 33773–33780. doi:10.1029/2001JD900054

Barker, J.D., Sharp, M.J., Fitzsimons, S.J., and Turner, R.J. (2006) Abundance and dynamics of dissolved organic carbon in glacier systems. *Arct Antarct Alp Res* **38:** 163–172.

Barrand, N.E., James, T.D., and Murray, T. (2010) Spatiotemporal variability in elevation changes of two high-Arctic valley glaciers. *J Glaciol* **56:** 771–780.

Berney, M., Hammes, F., Bosshard, F., Weilenmann, H.-U., and Egli, T. (2007) Assessment and interpretation of bacterial viability by using the LIVE/DEAD BacLight kit in combination with flow cytometry. *Appl Environ Microbiol* **73:** 3283–3290.

Björnsson, H., Gjessing, Y., Hamran, S.-E., Hagen, J.O., Liestøl, O., Pálsson, F., and Erlingsson, B. (1996) The thermal regime of sub-polar glaciers mapped by multi-frequency radio-echo sounding. *J Glaciol* **42:** 23–32.

Bøggild, C.E., Brandt, R.E., Brown, K.J., and Warren, S.G. (2010) The ablation zone in northeast Greenland: ice types, albedos, and impurities. *J Glaciol* **56:** 101–113.

Boulos, L., Prevos, M., Barbeau, B., Coallier, J., and Desjardins, R. (1999) LIVE/DEAD BacLight: application of a new rapid staining method for direct enumeration of viable and total bacteria in drinking water. *J Microbiol Methods* **37:** 77–86.

Boyd, E.S., Skidmore, M., Mitchell, A.C., Bakermans, C., and Peters, J.W. (2010) Methanogenesis in subglacial sediments. *Environ Microbiol* **2:** 685–692.

Brussaard, C.P.D., Marie, D., and Bratbak, G. (2000) Flow cytometric detection of viruses. *J Virol Methods* **85:** 175–182.

Christensen, J.H., Hewitson, B., Busuioc, A., Chen, A., Gao, X., Held, I., *et al*. (2007) Regional climate projections. In *Climate Change 2007: The Physical Science Basis Contribution of Working Group I to the Fourth Assessment Report of the Intergovernmental Panel on Climate Change*. Solomon, S., Qin, D., Manning, M., Chen, Z., Marquis, M., Averyt, K.B., *et al*. (eds). Cambridge, UK: Cambridge University Press, pp. 847–940.

Christner, B.C., Mosley-Thompson, E., Thompson, L.G., Zagorodnov, V., Sandman, K., and Reeve, J.N. (2000) Recovery and identification of viable bacteria immured in glacial ice. *Icarus* **144:** 479–485.

Christner, B.C., Kvitko, B.H., and Reeve, J.N. (2003a) Molecular identification of bacteria and eukarya inhabiting an Antarctic cryoconite hole. *Extremophiles* **7:** 177–183.

Christner, B.C., Mosley-Thompson, E., Thompson, L.G., and Reeve, J.N. (2003b) Bacterial recovery from ancient ice. *Environ Microbiol* **5:** 433–436.

Chuvochina, M.S., Marie, D., Chevaillier, S., Petit, J.-R., Normand, P., Alekhina, I.A., and Bulat, S.A. (2011) Community variability of bacteria in alpine snow (Mont Blanc) containing Saharan dust deposition and their snow colonisation potential. *Microbes Environ* **26:** 237–247.

Collier, J.L., and Campbell, L. (1999) Flow cytometry in molecular aquatic ecology. *Hydrobiologia* **401:** 33–53.

Dancer, S.J., Shears, P., and Platt, D.J. (1997) Isolation and characterization of coliforms from glacial ice and water in Canada's High Arctic. *J Appl Microbiol* **82:** 597–609.

Davey, H.M., and Hexley, P. (2011) Red but not dead? Membranes of stressed *Saccharomyces cerevisiae* are permeable to propidium iodide. *Environ Microbiol* **13:** 163–171.

Day, T. (1976) On the precision of salt dilution gauging. *J Hydrol* **31:** 293–306.

DiMarco, A.A., Bobik, T.A., and Wolfe, R.S. (1990) Unusual coenzymes of methanogenesis. *Annu Rev Biochem* **59:** 355–394.

Edwards, A., Anesio, A.M., Rassner, S.M., Sattler, B., Hubbard, B., Perkins, W.T., *et al*. (2011) Possible interactions between bacterial diversity, microbial activity and supraglacial hydrology of cryoconite holes in Svalbard. *ISME J* **5:** 150–160.

Fagerbakke, K., Heldal, M., and Norland, S. (1996) Content of carbon, nitrogen, oxygen, sulfur and phosphorus in native aquatic and cultured bacteria. *Aquat Microb Ecol* **10:** 15–27.

Felip, M., Andreatta, S., Sommaruga, R., Straskrábová, V., and Catalan, J. (2007) Suitability of flow cytometry of estimating bacterial biovolume in natural plankton samples: comparison with microscopy data. *Appl Environ Microbiol* **73:** 4508–4514.

Fukuda, R., Ogawa, H., Nagata, T., and Koike, I. (1998) Direct determination of carbon and nitrogen contents of natural bacterial assemblages in marine environments. *Appl Environ Microbiol* **64:** 3352–3358.

Goossens, D. (2005) Quantification of the dry aeolian deposition of dust on horizontal surfaces: an experimental comparison of theory and measurements. *Sedimentology* **52:** 859–873.

Hall, D.J., and Waters, R.A. (1986) An improved, readily available dustfall gauge. *Atmos Environ* **20:** 219–222.

Hambrey, M.J., Murray, T., Glasser, N.F., Hubbard, A., Hubbard, B., Stuart, G., *et al*. (2005) Structure and changing dynamics of a polythermal valley glacier on a centennial timescale: Midre Lovénbreen, Svalbard. *J Geophys Res* **110** (F01006). doi:10.1029/2004JF000128

Hammes, F., and Egli, T. (2010) Cytometric methods for measuring bacteria in water: advantages, pitfalls and applications. *Anal Bioanal Chem* **397:** 1083–1095.

Hawes, T.C. (2008) Aeolian fallout on recently deglaciated terrain in the high Arctic. *Polar Biol* **31:** 295–301.

Hodson, A., Kohler, J., Brinkhaus, M., and Wynn, P. (2005) Multi-year water and surface energy budget of a high-latitude polythermal glacier: evidence for overwinter water storage in a dynamic subglacial reservoir. *Ann Glaciol* **42:** 42–46.

Hodson, A., Anesio, A.M., Ng, F., Watson, R., Quirk, J., Irvine-Fynn, T., *et al*. (2007) A glacier respires: quantifying the distribution and respiration CO_2 flux of cryoconite across an entire Arctic supraglacial ecosystem. *J Geophys Res* **112** (G04S36). doi:10.1029/2004JF000128

Hodson, A.J., Anesio, A.M., Tranter, M., Fountain, A.G., Osborn, A.M., Priscu, J., *et al*. (2008) Glacial ecosystems. *Ecol Monogr* **78:** 41–67.

Hodson, A., Cameron, K., Bøggild, C., Irvine-Fynn, T., Langford, H., Pearce, D., and Banwart, S. (2010) The structure, biogeochemistry and formation of cryoconite aggregates upon an Arctic valley glacier; Longyearbreen, Svalbard. *J Glaciol* **56:** 349–362.

Hood, E., Fellman, J., Spencer, R.G.M., Hernes, P.J., Edwards, R., D'Amore, D., and Scott, D. (2009) Glaciers as a source of ancient and labile organic matter to the marine environment. *Nature* **462:** 1044–1047.

Hubbard, B.P., Sharp, M.J., Willis, I.C., Nielsen, M.K., and Smart, C.C. (1995) Borehole water-level varitions and the structure of the subglacial hydrological system of Haut Glacier d'Arolla, Valais, Switzerland. *J Glaciol* **41:** 572–583.

Irvine-Fynn, T.D.L. (2008) Modelling runoff from the maritime Arctic cryosphere: water storage and routing at Midtre Lovénbreen. PhD Thesis. Sheffield, UK: University of Sheffield, pp. 384.

Irvine-Fynn, T.D.L., and Hodson, A.J. (2010) Biogeochemistry and dissolved oxygen dynamics at a subglacial upwelling, Midtre Lovénbreen, Svalbard. *Ann Glaciol* **51:** 41–46.

Irvine-Fynn, T.D.L., Hodson, A.J., Kohler, J., Porter, P.R., and Vatne, G. (2005) Dye tracing experiments at Midre Lovénbreen, Svalbard: preliminary results and interpretations. In *Glacier Caves and Glacial Karst in High Mountains and Polar Regions: Proceedings 7th GLACKIPR Conference, Sept 2005, Azau*. Mavlyudov, B.R. (ed.). Moscow, Russia: Institute of Geography, Russian Academy of Sciences, pp. 36–43.

Irvine-Fynn, T.D.L., Bridge, J.W., and Hodson, A.J. (2011) In situ quantification of supraglacial cryoconite morphodynamics using time-lapse imaging: an example from Svalbard. *J Glaciol* **57:** 651–657.

Kamiya, E., Izumiyama, S., Nishimura, M., Mitchell, J.G., and Kogure, K. (2007) Effects of fixation and storage on flow cytometric analysis of marine bacteria. *J Oceanogr* **63:** 101–112.

Kattsov, V.M., Källén, E., Cattle, H., Christensen, J., Drange, H., Hanssen-Bauer, I., *et al*. (2005) Future climate change: modeling and scenarios for the Arctic. In *Arctic Climate Impact Assessment*. Cambridge, UK: Cambridge University Press, pp. 99–150.

Kell, D.B., Ryder, H.M., Kaprelyants, A.S., and Westerhoff, H.V. (1991) Quantifying heterogeneity: flow cytometry of bacterial cultures. *Antonie Van Leeuwenhoek* **60:** 145–158.

Keller, H.M. (1969) Measuring stream discharge using the dye dilution method (chemical gauging). In *Water and Soil Division: Hydrological Publication 2*. Wellington, New Zealand: New Zealand Ministry of Works.

Klauth, P., Wilhelm, R., Klumpp, E., Poschen, L., and Groeneweg, J. (2004) Enumeration of soil bacteria with the green fluorescent nucleic acid dye Sytox green in the presence of soil particles. *J Microbiol Methods* **59:** 189–198.

Kohler, J., James, T.D., Murray, T., Nuth, C., Brandt, O., Barrand, N.E., *et al*. (2007) Acceleration in thinning rate on western Svalbard glaciers. *Geophys Res Lett* **34** (L18502). doi:10.1029/2007GL030681

Kohshima, S., Seko, K., and Yoshimura, Y. (1993) Biotic acceleration of glacier melting in Yala Glacier, Langtant region, Nepal Himalaya. *IAHS Publ* **218:** 309–316.

Konzelmann, T., and Braithwaite, R.J. (1995) Variations of ablation, albedo and energy balance at the margin of the Greenland ice sheet, Kronprins Christian Land, eastern north Greenland. *J Glaciol* **41:** 174–182.

Langford, H., Hodson, A., Banwart, S., and Bøggild, C. (2010) The microstructure and biogeochemistry of Arctic cryoconite granules. *Ann Glaciol* **51:** 87–94.

Lebaron, P., Parthuisot, N., and Catala, P. (1998) Comparison of blue nucleic acid dyes in aquatic systems. *Appl Environ Microbiol* **64:** 1725–1730.

Liu, Y., Yao, T., Jiao, N., Kang, S., Xu, B., Zeng, Y., *et al*. (2009) Bacterial diversity in the snow over Tibetan Plateau Glaciers. *Extremophiles* **13:** 411–423.

Mader, H.M., Pettitt, M.E., Wadham, J.L., Wolff, E.W., and Parkes, R.J. (2006) Subsurface ice as a microbial habitat. *Geology* **34:** 169–172.

Mahowald, N.M., Kloster, S., Engelstaedter, S., Moore, J.K., Mukhopadhyay, S., McConnell, J.R., *et al*. (2010) Observed 20th century desert dust variability: impact on climate and biogeochemistry. *Atmos Chem Phys Discuss* **10:** 10875–10893.

Marie, D., Simon, N., and Vaulot, D. (2005) Phytoplankton cell counting by flow cytometry. In *Algal Culturing Techniques*. Andersen, R.A. (ed.). London, UK: Phycological Society of America & Elsevier Academic Press, pp. 253–268.

Mindl, B., Anesio, A.M., Meirer, K., Hodson, A.J., Laybourn-Parry, J., Sommaruga, R., and Sattler, B. (2007) Factors influencing bacterial dynamics along a transect from supraglacial runoff to proglacial lakes of a high Arctic glacier. *FEMS Microbiol Ecol* **59:** 307–317.

Miteva, V., Teacher, C., Sowers, T., and Brenchley, J. (2009) Comparison of the microbial diversity at different depths of the GISP2 Greenland ice core in relationship to deposition climates. *Environ Microbiol* **11:** 640–656.

Miteva, V.I., and Brenchley, J.E. (2005) Detection and isolation of ultrasmall microorganisms from a 120,000-year-old Greenland glacier ice core. *Appl Environ Microbiol* **71:** 7806–7818.

Morgan-Kiss, R.M., Priscu, J.C., Pocock, T., Gudynaite-Savitch, L., and Huner, N.P.A. (2006) Adaptation and acclimation of photosynthetic microorganisms to permanently cold environments. *Microbiol Mol Biol Rev* **70:** 222–252.

Morono, Y., Terada, T., Masui, N., and Inagaki, F. (2009) Discriminative detection and enumeration of microbial life in marine subsurface sediments. *ISME J* **3:** 503–511.

Mueller, D.R., and Pollard, W.H. (2004) Gradient analysis of cryoconite ecosystems from two polar glaciers. *Polar Biol* **27:** 66–74.

Müller, F., and Keeler, C.M. (1969) Errors in short-term ablation measurements on melting ice surfaces. *J Glaciol* **8:** 91–105.

Munro, D.S. (2011) Delays of supraglacial runoff from differently defined microbasin areas on the Peyto Glacier. *Hydrol Processes* **25:** 2983–2994.

Nebe-von-Caron, G. (2009) Standardization in microbial cytometry. *Cytometry* **75A:** 86–89.

Phe, M.-H., Dossot, M., Guilloteau, H., and Block, J.-C. (2007) Highly chlorinated *Escherichia coli* cannot be stained by propidium iodide. *Can J Microbiol* **53:** 664–670.

Price, P.B. (2007) Microbial life in glacial ice and implications for a cold origin of life. *FEMS Microbiol Ecol* **59:** 217–231.

Price, P.B., Rohde, R.A., and Bay, R.C. (2009) Fluxes of microbes, organic aerosols, dust, sea-salt Na ions, non-sea-salt Ca ions, and methanesulfonate onto Greenland and Antarctic ice. *Biogeosciences* **6:** 479–486.

Priscu, J.C., and Christner, B.C. (2004) Earth's icy biosphere. In *Microbial Diversity and Bioprospecting*. Bull, A.T. (ed.). Washington, DC, USA: American Society for Microbiology, pp. 130–145.

Purwantini, E., Gillis, T.P., and Daniels, L.F.M.L. (1997) Presence of F_{420}-dependent glucose-6-phosphate dehydrogenase in *Mycobacterium* and *Nocardia* species, but absence from *Streptomyces* and *Corynebacterium* species and methanogenic Archaea. *FEMS Microbiol Lett* **146:** 129–134.

Radić, V., and Hock, R. (2010) Regional and global volumes of glaciers derived from statistical upscaling of glacier inventory data. *J Geophys Res* **115** (F01010). doi:10.1029/2009JF001373

Rassner, S.M. (2009) Influences of bacterial resources on the dynamics of virus bacterium interactions in aquatic ecosystems. PhD Thesis. Aberystwyth, UK: Aberystwyth University, pp. 255.

Rogers, S.O., Starmer, W.T., and Castello, J.D. (2004) Recycling of pathogenic microbes through survival in ice. *Med Hypotheses* **63:** 773–777.

Röthlisberger, H. (1972) Water pressure in intra- and subglacial channels. *J Glaciol* **11:** 177–203.

Salerno, M.B., Logan, B.E., and Velegol, D. (2004) Importance of molecular details in predicting bacterial adhesion to hydrophobic surfaces. *Langmuir* **20:** 10625–10629.

Säwström, C., Mumford, P., Marshall, W., Hodson, A., and Laybourn-Parry, J. (2002) The microbial communities and primary productivity of cryoconite holes in an Arctic glacier (Svalbard 79°N). *Polar Biol* **25:** 591–596.

Segawa, T., Miyamoto, K., Ushida, K., Agata, K., Okada, N., and Koshima, S. (2005) Seasonal change in bacterial flora and biomass in mountain snow from the Tateyama Mountains, Japan, analyzed by 16S rRNA gene sequencing and real-time PCR. *Appl Environ Microbiol* **71:** 123–130.

Shellenbergen, K., and Logan, B.E. (2002) Effect of molecular scale roughness of glass beads on colloidal and bacterial deposition. *Environ Sci Technol* **36:** 184–189.

Sheridan, P.P., Miteva, V.I., and Brenchley, J.E. (2003) Phylogenetic analysis of anaerobic psychrophilic enrichment cultures obtained from a Greenland glacier ice core. *Appl Environ Microbiol* **69:** 2153–2160.

Simon, M., and Azam, F. (1989) Protein-content and protein-synthesis rates of planktonic marine-bacteria. *Mar Ecol Prog Ser* **51:** 201–213.

Sobota, I. (2009) The near-surface ice thermal structure of the Waldemarbreen, Svalbard. *Pol Polar Res* **30:** 317–338.

Sow, M., Goossens, D., and Rajot, J.L. (2006) Calibration of the MDCO dust collector and of four versions of the inverted frisbee dust deposition sampler. *Geomorphology* **82:** 360–375.

Stibal, M., Telling, J., Cook, J., Mak, K.M., Hodson, A., and Anesio, A.M. (2012) Environmental controls on microbial abundance and activity on the Greenland Ice Sheet: a multivariate analysis approach. *Microb Ecol* **63:** 74–84.

Sunamura, M., Maruyama, A., Tsuji, T., and Kurane, R. (2003) Spectral imaging detection and counting of microbial cells in marine sediment. *J Microbiol Methods* **53:** 57–65.

Takeuchi, N. (2002) Optical characteristics of cryoconite (surface dust) on glaciers: the relationship between light absorbency and the property of organic matter contained in the cryoconite. *Ann Glaciol* **34:** 409–414.

Takeuchi, N. (2009) Temporal and spatial variations in spectral reflectance and characteristics of surface dust on Gulkana Glacier, Alaska Range. *J Glaciol* **55:** 701–709.

Takeuchi, N., Kohshima, S., and Seko, K. (2001a) Structure, formation, and darkening process of albedo-reducing material (cryoconite) on a Himalayan glacier: a granular algal mat growing on the glacier. *Arct Antarct Alp Res* **33:** 115–122.

Takeuchi, N., Kohshima, S., Goto-Azuma, K., and Koerner, R. (2001b) Biological characteristics of dark colored material (cryoconite) on Canadian Arctic glaciers (Devon and Penny ice caps). *Mem Natl Inst Polar Res* **54:** 495–505.

Takeuchi, N., Nishiyama, H., and Li, Z. (2010) Structure and formation process of cryoconite granules on Ürümqi glacier No. 1, Tien Shan, China. *Ann Glaciol* **51:** 9–14.

Telling, J., Anesio, A.M., Hawkings, J., Tranter, M., Wadham, J.L., Hodson, A.J., *et al*. (2010) Measuring rates of gross photosynthesis and net production in cryoconite holes: a comparison of field methods. *Ann Glaciol* **51:** 153–162.

Tieber, A., Lettner, H., Bossew, P., Hubmer, A., Sattler, B., and Hofmann, W. (2009) Accumulation of anthropogenic radionuclides in cryoconite on Alpine glaciers. *J Environ Radioact* **100:** 590–598.

Tranter, M., Huybrechts, P., Munhoven, G., Sharp, M.J., Brown, G.H., Jones, I.W., *et al*. (2002) Direct effect of ice sheets on terrestrial bicarbonate, sulphate and base cation fluxes during the last glacial cycle: minimal impact on atmospheric CO_2 concentrations. *Chem Geol* **190:** 33–44.

Troussellier, M., Courties, C., and Zettemaier, S. (1995) Flow cytometric analysis of coastal lagoon bacterioplankton and picophytoplankton: fixation and storage effects. *Estuar Coast Shelf Sci* **40:** 621–633.

Tung, H.C., Bramall, N.E., and Price, P.B. (2005) Microbial origin of excess methane in glacial ice and implications for life on Mars. *Proc Natl Acad Sci USA* **102:** 18292–18296.

Tung, H.C., Price, P.B., Bramall, N.E., and Vrdoljak, G. (2006) Microorganisms metabolizing on clay 10 grains in 3-km-deep Greenland basal ice. *Astrobiology* **6:** 69–86.

Turley, C.M., and Hughes, D.J. (1992) Effects of storage on direct estimates of bacterial numbers of preserved seawater samples. *Deep Sea Res A* **39:** 375–394.

Vincent, W.F. (2007) Cold tolerance in cyanobacteria and life in the cryosphere. In *Cellular Origin, Life in Extreme Habitats and Astrobiology: Algae and Cyanobacteria in Extreme*

Enviromments. Seckbach, J. (ed.). Dordrecht, the Netherlands: Springer, pp. 287–301.
Vrede, K., Heldal, M., Norland, S., and Bratbak, G. (2002) Elemental composition (C, N, P) and cell volume of exponentially growing and nutrient-limited bacterioplankton. *Appl Environ Microbiol* **68:** 2965–2971.
Wadham, J.L., and Nuttall, A.-M. (2002) Multiphase formation of superimposed ice during a mass-balance year at a maritime high-Arctic glacier. *J Glaciol* **48:** 545–551.
Walker, F. (1931) Formaldehyde and its polymers. *Ind Eng Chem* **23:** 1220–1222.
Wang, Y., Hammes, F., Boon, N., and Egli, M. (2007) Quantification of the filterability of freshwater bacteria through 0.45, 0.22, and 0.1 μm pore size filters and shape-dependent enrichment of filterable bacterial communities. *Environ Sci Technol* **41:** 7080–7086.
Wang, Y., Hammes, F., De Roy, K., Verstraete, W., and Boon, N. (2010) Past, present and future applications of flow cytometry in aquatic microbiology. *Trends Biotechnol* **28:** 416–424.
Weinbauer, M.G., Beckmann, C., and Höfle, M.G. (1998) Utility of green fluorescent nucleic acid dyes and aluminium oxide membrane filters for rapid epifluorescence enumeration of soil and sediment bacteria. *Appl Environ Microbiol* **64:** 5000–5003.
Wharton, R.A., McKay, C.P., Simmons, G.M., and Parker, B.C. (1985) Cryoconite holes on glaciers. *BioScience* **35:** 499–503.
Whitman, W.B., Coleman, D.C., and Wiebe, W.J. (1998) Prokaryotes: the unseen majority. *Proc Natl Acad Sci USA* **95:** 6578–6583.
Wynn, P.M., Hodson, A.J., Heaton, T.H.E., and Chenery, S.R. (2007) Nitrate production beneath a High Arctic glacier, Svalbard. *Chem Geol* **244:** 88–102.
Yentsch, C.M., Horan, P.K., Muirhead, K., Dortch, Q., Haugen, E., Legendre, L., *et al*. (1983) Flow cytometry and cell sorting: a technique for analysis and sorting of aquatic particles. *Limnol Oceanogr* **28:** 1275–1280.

Supporting information

Additional Supporting Information may be found in the online version of this article:

Fig. S1. Example scatter plots from FCM showing contrast between (a) unstained and (b) stained response to blue (488 nm) laser excitation, highlighting the SGII shift in green fluorescence and a threshold ($\sim 10^2$ DN) for separating biological and non-biological particulates for a stream sample taken on DOY196. The threshold was defined from samples in which autofluorescent particles appeared absent. Panel c illustrates the SSC vs. FSC scatter plot for biological particles in a supraglacial stream sample and the size classification boundaries derived independently from the use of a pseudo-blank sample containing beads.

Please note: Wiley-Blackwell are not responsible for the content or functionality of any supporting materials supplied by the authors. Any queries (other than missing material) should be directed to the corresponding author for the article.